

Laboratori Nazionali di Frascati

LNF-66/53

S. Costa, S. Ferroni, V. G. Gracco, E. Silva and C. Schaerf:  
PHOTONEUTRON PRODUCTION FROM THE PROTON AT  
HIGH ENERGY.

Nuovo Cimento 45, 696 (1966)

## Photoneutron Production from the Proton at High Energy.

S. COSTA

*Istituto di Fisica dell'Università - Torino*

S. FERRONI, V. G. GRACCO, and E. SILVA

*Ecole Normale Supérieure, Laboratoire de l'Accélérateur Linéaire - Orsay*

C. SCHÄERF

*Ecole Normale Supérieure, Laboratoire de l'Accélérateur Linéaire - Orsay  
Laboratori Nazionali di Frascati del CNEN - Frascati*

(ricevuto l'11 Maggio 1966)

**Summary.** — The total neutron yield from the ( $\gamma$ , n) reaction in hydrogen has been measured as a function of the energy of the primary electron using the bremsstrahlung beam from the Orsay Linear Electron Accelerator. The yield has been interpreted as a contribution from single and double pion photoproduction in hydrogen. Close to threshold the results are consistent with the theoretical prediction of CGLN for single pion photoproduction. In the energy region (250  $\div$  450) MeV the results are consistent with the experimentally measured values of the total positive-pion photoproduction cross-section. At higher energies the results indicate a higher yield than previously anticipated for double pion photoproduction in the particular channel  $\gamma + p \rightarrow n + \pi^+ + \pi^0$ .

### 1. – Introduction.

In the field of photonuclear reaction, the measurements of total neutron cross-sections are commonly performed by means of so-called thermalized neutron detectors. These are suitable modifications of the well known Hanson-McKibben « long counter », firstly employed by HALPERN, MANN and MATHAUS<sup>(1)</sup>.

<sup>(1)</sup> J. HALPERN, A. K. MANN and R. NATHANS *Rev. Sci. Instr.*, **23**, 678 (1952).

We have used this technique, well exploited in low-energy nuclear physics to study the meson photoproduction on hydrogen. In particular, the measurement of the  $\gamma + p \rightarrow \pi^+ + n$  total cross-section has been accomplished near threshold. In this energy range, there are some angular-distribution data obtained with photographic emulsions or diffusion chamber. The only existing measurement of the total cross-section is the one performed with a bubble chamber (2). In the present work, the first results obtained with counters are reported.

Moreover, the total cross-section of the  $\gamma + p \rightarrow \pi^+ + \pi^0 + n$  process has been measured between threshold and 700 MeV.

## 2. - Experimental apparatus.

**2.1. Target and neutron detector.** - Figure 1 shows the experimental layout. The electron beam, after striking on an Al radiator (0.01 radiation lengths), is magnetically deflected into a beam catcher. The « bremsstrahlung » produced,

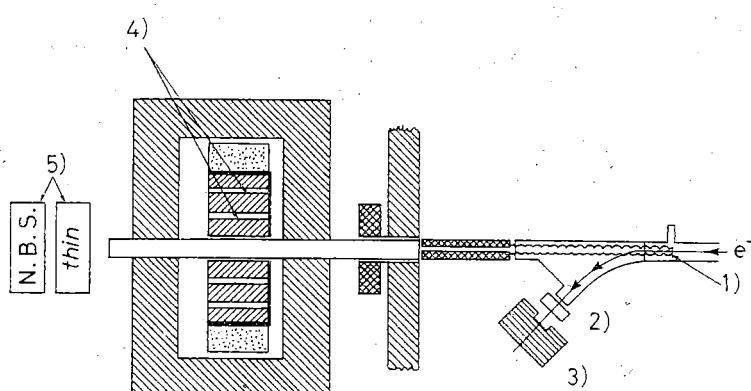


Fig. 1. Layout of the experimental apparatus: 1) radiator; 2) S.E.M.; 3) beam catcher; 4)  $\text{BF}_3$  counters; 5) ionization chambers; concrete; paraffin; lead; water +  $\text{H}_3\text{BO}_3$ ; cadmium.

before it reaches the target, traverses a 2m long, Pb collimator so that on the back side of the target the diameter of the  $\gamma$ -ray beam is about 4 cm. The target itself is a 9.2 m long steel tube ( $\varnothing = 10$  cm), closed at the two ends by Dural windows 5/10 mm thick, filled with gaseous  $\text{H}_2$  at 18 atm pressure. To measure the energy carried by the  $\gamma$ -ray beam two ionization chambers have been placed beyond the target: the first one is a thin chamber filled with hydrogen

(2) G. ASCOLI, G. L. GOLDWASSER, U. E. KRUSE, J. SIMPSON and W. P. SWANSON: *Proceedings of the Sienna Conference*, vol. 1 (1964), p. 485.

at atmospheric pressure; the second one is a conventional NBS P2 sealed-off chamber, with a thick Dural converter in front, and filled with dry air.

The neutron detector, already described elsewhere in more details <sup>(3)</sup>, has

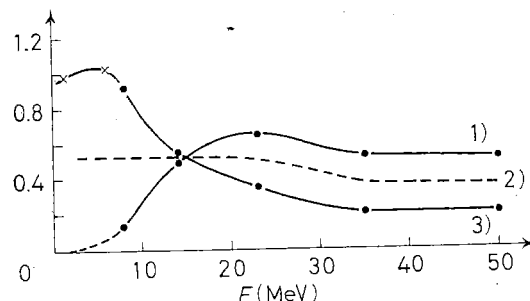


Fig. 2. – Neutron detection efficiency as function of the neutron energy as obtained from a Monte Carlo calculation: 1)  $11\epsilon(41; E)$ ; 2)  $(11\epsilon(41; E) + \epsilon(11.2; E))/2$ ; 3)  $\epsilon(11.2; E)$ .

surrounds completely the detector and, in front of the detector itself, by a block 50 cm thick of paraffin followed by a suitable cadmium sheet.

As a Monte Carlo calculation has shown <sup>(4)</sup> the inner counters (those 20 cm far from the axis) detect mainly neutrons whose energy is below 15 MeV, while the outer ones, neutrons with energy above 10 MeV (Fig. 2). By properly adding the countings of the two groups of counters one obtains a detector with the required constant efficiency.

**2.2. Electronics.** – The electronic apparatus, whose block diagram is shown in Fig. 3, can be divided in two main parts: the detecting and the counting ones. The former is composed by the  $BF_3$  counters (Type 73 Ne 40/5), each one followed by a shaper-amplifier, and a mixing circuit; the latter includes linear gates and scalers. From the preamplifier and the short-circuited delay-line shaper, pulses – 5 V high and 0.5  $\mu$ s wide are obtained, and in the case of the 7 external counters they are sent to an emitter follower OR circuit. The pulses from the internal counter and from the mixer are counted separately through a linear gate opened for 400  $\mu$ s, 20  $\mu$ s after the beam. The delayed gate triggering is provided by a synchronous pulse from the Linac. The neutron

<sup>(3)</sup> G. R. BISHOP, S. COSTA, S. FERRONI, R. MALVANO and G. RICCO *Nuovo Cimento*, **42** B, 157 (1966).

<sup>(4)</sup> A. MAGGIOLI and G. RICCO: *Monte Carlo calculations for a fast neutron counter*, INFN/BE-64/2 (1964); In performing the calculation the authors have taken into account the following processes: elastic scattering on C and H; inelastic scattering; ( $n, 2n$ ) reactions and neutron capture; L. PALMIERI and G. RICCO: *Nucl. Instr. and Meth.*, **33**, 120 (1965).

counting rate *vs.* time has an exponentially decreasing trend, both for internal and external counters (see *e.g.* Fig. 2 of ref. (5)). The neutron «mean lives»  $\tau_n$  are however different:  $(160 \pm 3) \mu\text{s}$  and  $(187 \pm 3) \mu\text{s}$ , respectively. There

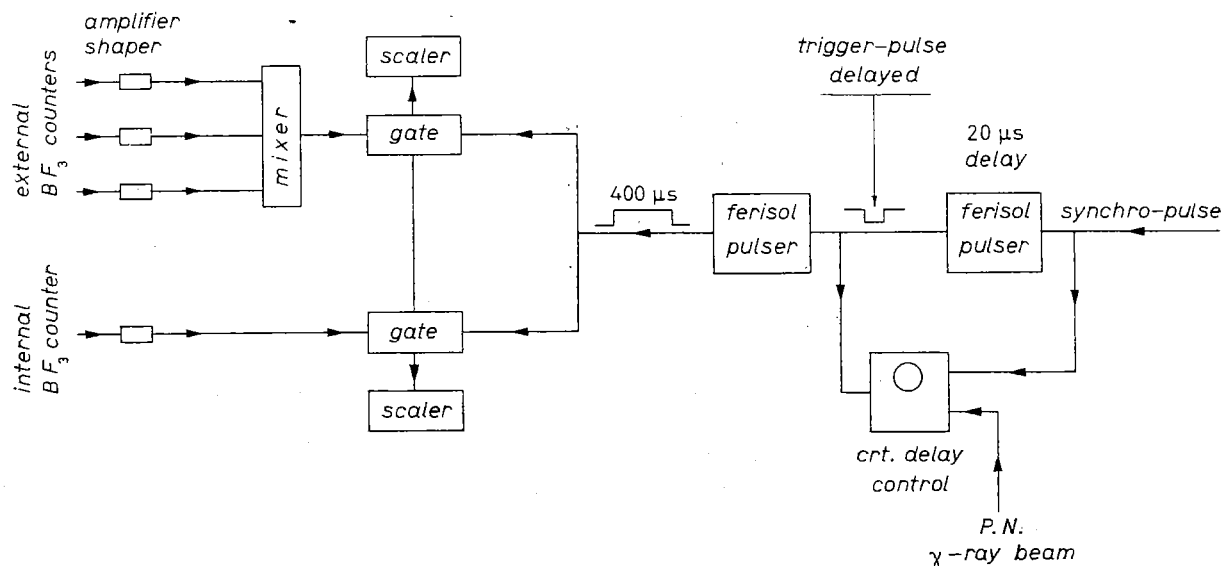


Fig. 3. – Block diagram of electronics of detection system.

are therefore two possible sources of error, one depending on slight changes in shape of the  $\gamma$ -ray pulses which introduce an incertitude in the gate triggering time, and the other connected with the different values of efficiency ratio (external over internal counter) one obtains with countinuous and with pulsed neutron sources. The first type of error is of the order of duration of the  $\gamma$ -ray pulse/ $\tau_n$ ) (see ref. (6)) *i.e.*  $\approx 0.5/160$  and has been therefore constantly neglected. The second one is systematic and has been taken into account.

### 3. – An analysis of experimental data.

The yield curve relative to the  $\pi^+$  photoproduction on hydrogen has been measured from 140 up to 700 MeV. The  $\gamma$  radiator has been chosen sufficiently thin not to have too serious distortions in the bremsstrahlung spectrum. At all energies, the yield points have been normalized to the NBS chamber readings and continuously checked with the response of the thin ionization chamber. The statistical error on the experimental points only seldom exceeded 1%.

The impurity of the  $\text{H}_2$  target was the main source of background. The presence of  $\text{D}_2$  and  $\text{H}_2\text{O}$  impurities gives an unwanted contribution to the yield

(5) G. C. BONAZZOLA and S. COSTA: *Nucl. Instr. and Meth.*, **28**, 274 (1964).

(6) S. COSTA and S. FERRONI: *Nucl. Instr. and Meth.*, **17**, 145 (1962).

points which has been subtracted by measuring the rather flat photodisintegration yield between 90 and 140 MeV, and then linearly extrapolating these points above the photoproduction threshold. The facilities of the 1.3 GeV Orsay linac have been exploited to explore the energy range ( $90 \simeq 700$ ) MeV.

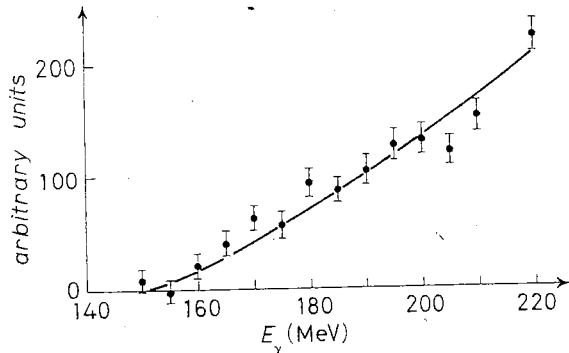


Fig. 4. — The experimental results near threshold are compared with the theoretical yield function calculated from the theory of C.G.L.N.: • experimental points; — C.G.L.N. theory.

which is shown (dashed line) in Fig. 2. In Fig. 4, the background has been subtracted as explained above. By comparing our data between 210 and

In the «low»-energy range ( $(90 \div 270)$  MeV) the runs have been performed using only the last section of the linac, which is provided with an independent injection system. The full linac has been used to take data between 250 and 700 MeV.

In Fig. 4 the yield points relative to the low-energy region are shown in arbitrary units. It should be emphasized that these points represent the contribution from the internal and the external  $\text{BF}_3$  counters, properly added together to obtain the efficiency curve

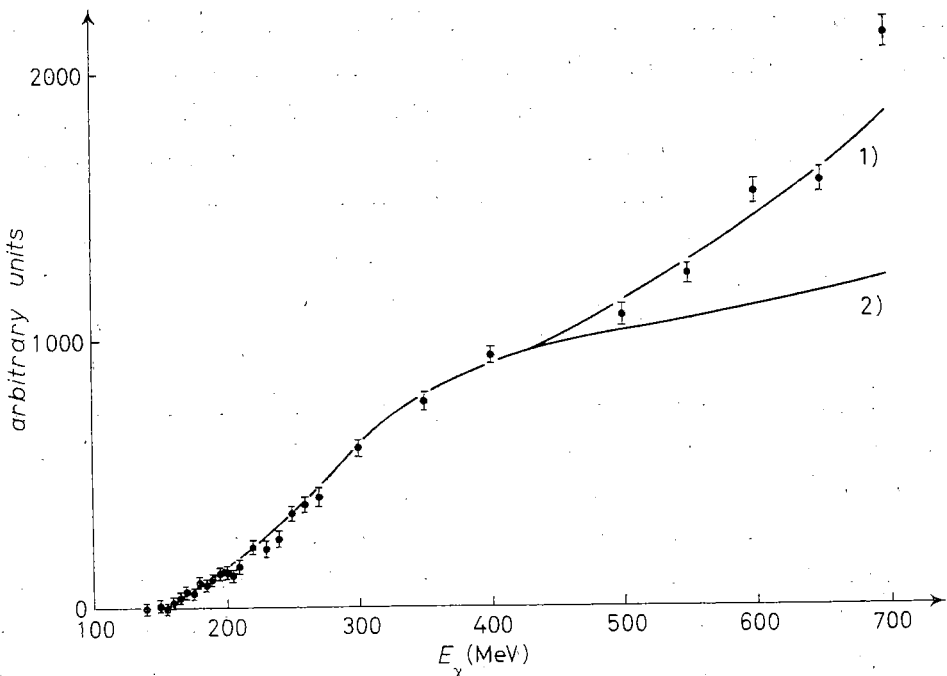


Fig. 5. — The experimental results at high energy are compared with the calculated yield function assuming measured values of the single-pion photoproduction cross-section and measured values, properly normalized, of the total cross-section for the process  $\gamma + p \rightarrow p + \pi^+ + \pi^-$ . 1)  $\gamma + p \rightarrow n + \pi^+ + 4(\gamma + p \rightarrow p + \pi^+ + \pi^-)$ ; 2)  $\gamma + p \rightarrow n + \pi^+$ .

270 MeV with those, reported in ref. (7) on the total cross-section of the reaction  $\gamma + p \rightarrow n + \pi^+$  the low-energy points have been normalized, and a similar procedure has been adopted to give absolute values to the points in the «high-energy» region: here, the data between 300 and 400 MeV, where the two-pion photoproduction is supposed to be negligible (see ref. (7,8,9)) have been used. In Fig. 5 the curve (2) represents the yield of single-pion photoproduction.

As it can be seen, there is a very good agreement between the experimental points and the curve representing the excitation function of single-pion photoproduction up to 450 MeV; thereafter the experimental values begin to rise very steeply, according to the onset of the two reactions

$$(1) \quad \left\{ \begin{array}{l} a) \quad \gamma + p \rightarrow n + \pi^+ + \pi^0, \\ b) \quad \gamma + p \rightarrow p + \pi^+ + \pi^- . \end{array} \right.$$

To get a useful insight into our experimental results it is necessary to study in which way the two reactions *a*) and *b*) lead to neutron production and to evaluate the associated neutron multiplicity. Let us consider firstly reaction *a*). Beside those neutrons which are directly produced, there could be other neutrons, arising from nuclear interactions of the pions in the moderator. Actually:

1) Ionization energy losses in the paraffin rapidly reduce the  $\pi^+$  at rest, but, owing to their charge, no absorption process can occur. No neutrons are therefore produced in this way. On the other hand, capture in flight and inelastic scattering are completely negligible.

Moreover, the  $\gamma$  from the decay of the  $\pi^0$ 's might really give rise to neutrons through the  $(\gamma, n)$  reaction, but a simple calculation shows that this effect is not greater than 1 %. We can therefore conclude that an appreciable number of neutrons, beside the direct ones, is not associated with reaction *a*), and that the neutron multiplicity is in this case very nearly one.

2) In the case of reaction *b*) we have only to evaluate the neutron multiplicity associated with the capture of  $\pi^-$  at rest. When a  $\pi^-$  is captured by a nucleus, neutrons can be emitted either via a direct interaction or following an evaporative process.

(7) G. G. KÄLLÉN: *Elementary Particle Physics*.

(8) J. M. SELLEN, G. COCCONI, V. T. COCCONI and E. L. HART: *Phys. Rev.*, **113**, 1323 (1959); B. M. CHASAN, G. COCCONI, V. T. COCCONI and R. M. SCHECTMAN: *Phys. Rev.*, **119**, 811 (1960).

(9) J. V. ALLABY, H. L. LYNCH and D. M. RITSON: *Phys. Rev.*, **142**, 887 (1966).

*α) Direct emission.* The  $\pi^-$  is captured by a two-nucleon subsystem according to the following reactions;

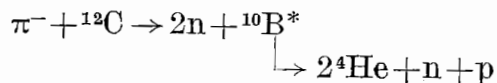


The ratio of the cross sections of the two reactions has been measured by OZAKI and coworkers (10) and found to be 5. The  $\frac{5}{6}$  of the  $\pi^-$ 's which are captured at rest by carbon nuclei, give therefore rise to 2 neutrons while  $\frac{1}{6}$  give rise to one neutron. The analogous « direct » process on  $H_2$  is negligible ( $< 0.1\%$ ). The neutron multiplicity associated with such direct processes is then

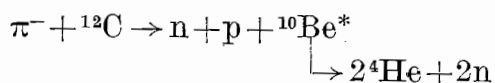
$$2 \cdot \frac{5}{6} + 1 \cdot \frac{1}{6} = 1.83 .$$

*β) Evaporative processes.* Following the direct emission of two nucleons the residual nucleus is indeed in an excited state and can de-excite emitting other neutrons, by means of an evaporative process.

In summary, one can guess what happens after the  $\pi^-$  is captured according with the reactions



or



The disintegration of  ${}^{10}B^*$  and  ${}^{10}Be^*$  have been studied in detail by CAMPOS VENUTI and MATTHIAE (11) and by AMMIRAJU and LEDERMANN (12) and by O'CONNELL and coworkers (13). From the above consideration it seems correct to associate to the  $\pi^-$  capture process a neutron multiplicity equal to three. This is in agreement with the measurements by ANDERSON *et al* (14) who find a neutron multiplicity equal to 2.8.

(10) S. OZAKI, R. WEINSTEIN, G. GLASS, E. LOH, L. NEIMALA and A. WATTENBERG: *Phys. Rev. Lett.*, **4**, 533 (1960).

(11) G. CAMPOS VENUTI and G. MATTHIAE: Report Istituto Superiore di Sanità ISS 62/21 (1962).

(12) P. AMMIRAJU and L. D. LEDERMANN: *Nuovo Cimento*, **4**, 281 (1956).

(13) J. O'CONNELL, P. DYAL and J. GOLDENBERG: *Phys. Rev.*, **116**, 173 (1959).

(14) H. ANDERSON, *et al.*: E.F.I.N.S. 73-56.

#### 4. – Interpretation of results.

In Figg. 4 and 5 are reported the experimental points between 150 and 700 MeV. The full line represents the integrated (over the bremsstrahlung spectrum) total cross-section of the reaction  $\gamma + p \rightarrow \pi^+ + n$  according to the CGLN (15,16) theory. The agreement, within the experimental errors, is very satisfactory.

Our results are moreover in complete agreement with the only existing measurement of the total  $\gamma + p \rightarrow n + \pi^+$  cross-section performed with a bubble chamber (2).

For the high-energy ( $> 300$  MeV) region, we try to interpret the experimental data by supposing, beside single photoproduction, the presence of double photoproduction.

In Table I the experimental values are compared with the function

$$Y = Y_1 + \lambda Y_2,$$

where

$\lambda$  free parameter to be determined from our experimental data;

$Y_1$  yield for single-pion photoproduction as obtained from the experimentally measured values of the total cross-section;

$Y_2$  yield for double-pion photoproduction as obtained from the experimental values of ref. (9).

$\lambda Y_2$  represents the contribution from reactions *a* and *b* of 1.

For  $\lambda$  we obtained the best fit value of  $\lambda = 4$ .

As the reaction (1b) is detected with a multiplicity of 3 and reaction 1a with a multiplicity of 1 our result is consistent with the ratio:

$$\frac{\sigma_{\text{tot}}(\gamma p \rightarrow \pi^+ \pi^0 n)}{\sigma_{\text{tot}}(\gamma p \rightarrow \pi^+ \pi^- p)} = 1.$$

This result is in agreement with the results of BLOCH and SANDS (17), FRIEDMAN and CROWE (18) and KUSUMEGI *et al.* (19) which have been obtained with different techniques.

(15) F. CHEW, M. L. GOLDBERGER, F. LOW and Y. NAMBU: *Phys. Rev.*, **106**, 1345 (1957).

(16) C. S. ROBINSON: *Tables of cross-sections for  $\pi^+$  photoproduction according to the theory of CGLN*, University of Illinois (1959).

(17) M. BLOCH and M. SANDS: *Phys. Rev.*, **108**, 1101 (1957); **113**, 305 (1959).

(18) R. M. FRIEDMAN and K. M. CROWE: *Phys. Rev.*, **105**, 1369 (1957).

(19) A. KUSUMEGI, Y. KOBAYASHI, Y. MURATA, H. SASAKI, K. TAKAMATSU and A. MASAIKE: *Proceedings of the International Symposium on Electron and Photon Interactions at High Energies*, vol. 2 (Hamburg, 1965), p. 253.

### 5. – Discussion.

We can try to interpret this result taking into account only the possible configurations of isotopic spin in the final state and introducing the hypothesis that the nucleon is always in a  $T = \frac{3}{2}$  state with one of the pions. In this way we can write for the two possible final states:

$$\begin{aligned} |\frac{1}{2}, \frac{1}{2}\rangle &= \frac{1}{\sqrt{2}} |\pi^-; N^{*++}\rangle - \frac{1}{\sqrt{3}} |\pi^0; N^{*+}\rangle + \frac{1}{\sqrt{6}} |\pi^+; N^{*0}\rangle = \\ &= \frac{1}{\sqrt{2}} |\pi^-; p, \pi^+\rangle - \frac{1}{\sqrt{3}} \left\{ \frac{1}{\sqrt{3}} |\pi^0; n, \pi^+\rangle + \right. \\ &\quad \left. + \sqrt{\frac{2}{3}} |\pi^0; p, \pi^0\rangle \right\} + \frac{1}{\sqrt{6}} \left\{ \frac{1}{\sqrt{3}} |\pi^+; p, \pi^-\rangle + \sqrt{\frac{2}{3}} |\pi^+; n, \pi^0\rangle \right\} = \\ &= \sqrt{\frac{8}{9}} |\pi^-, p, \pi^+\rangle - \frac{\sqrt{2}}{3} |\pi^0, p, \pi^0\rangle \end{aligned}$$

and

$$\begin{aligned} |\frac{3}{2}, \frac{1}{2}\rangle &= -\sqrt{\frac{2}{5}} |\pi^-; N^{*++}\rangle - \sqrt{\frac{1}{15}} |\pi^0, N^{*+}\rangle + \sqrt{\frac{8}{15}} |\pi^+, N^{*0}\rangle = \\ &= -\frac{1}{3} \sqrt{\frac{2}{5}} |\pi^-, p, \pi^+\rangle + \frac{1}{\sqrt{5}} |\pi^+, n, \pi^0\rangle - \sqrt{\frac{2}{45}} |\pi^0, p, \pi^0\rangle. \end{aligned}$$

Now using our experimental result we have:

$$\frac{\sigma(\gamma + p \rightarrow \pi^+ + \pi^0 + n)}{\sigma(\gamma + p \rightarrow \pi^+ + \pi^- + p)} = \left| + \frac{1}{\sqrt{5}} A_{\frac{1}{2}} \right|^2 / \left| \sqrt{\frac{8}{9}} A_{\frac{1}{2}} - \frac{1}{\sqrt{5}} \sqrt{\frac{2}{3}} A_{\frac{3}{2}} \right|^2 = 1,$$

from which we obtain

$$\frac{|A_{\frac{1}{2}}|}{|A_{\frac{3}{2}}|} = \begin{cases} 0.73, & \text{if } \cos \varphi = +1, \\ 0.45, & \text{if } \cos \varphi = 0, \\ 0.28, & \text{if } \cos \varphi = -1, \end{cases}$$

where  $\varphi$  is the relative phase of the two complex amplitudes  $A_{\frac{1}{2}}$  and  $A_{\frac{3}{2}}$ . From this results we can now calculate the ratio

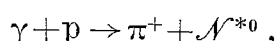
$$r = \frac{\sigma(\gamma + p \rightarrow \pi^+ + N^{*0})}{\sigma(\gamma + p \rightarrow \pi^- + N^{*++})} = \left| \frac{1}{\sqrt{6}} A_{\frac{1}{2}} + \sqrt{\frac{8}{15}} A_{\frac{3}{2}} \right|^2 / \left| \frac{1}{\sqrt{2}} A_{\frac{1}{2}} - \sqrt{\frac{2}{5}} A_{\frac{3}{2}} \right|^2,$$

which is equal to

$$r = \begin{cases} 0.8, & +1, \\ 1.1, & 0, \\ 0.54, & -1, \end{cases} \quad \text{if } \cos \varphi = \begin{cases} +1, \\ 0, \\ -1, \end{cases}$$

according to various possible choices of the phase  $\varphi$ .

This seems in serious contradiction with existing experimental data <sup>(9)</sup> which give no evidence for the reaction



Therefore we arrive at the conclusion that our previous hypothesis that the nucleon is always in a  $T = \frac{3}{2}$  state with one pion is invalid.

\* \* \*

It is a pleasure to thank Prof. BLANK-LAPIERRE for his hospitality at the Laboratoire de l'Accélérateur Linéaire where this experiment has been performed. We also thank Prof. S. FUBINI, Prof. P. LEHMANN, Prof. PEREZ Y JORBA and Dr. A. BOTTINO for many helpful discussions and the machine crew headed by L. BURNOD for the continuous and reliable operation of the machine.

#### RIASSUNTO

Si è misurata la resa totale di neutroni della reazione  $(\gamma, n)$  in idrogeno in funzione dell'energia del protone primario facendo uso del fascio di bremsstrahlung dell'Acceleratore lineare di elettroni di Orsay. La resa è stata interpretata come il contributo della fotoproduzione singola e doppia di pioni in idrogeno. Vicino alla soglia i risultati sono concordanti con la predizione teorica di GGLN per la fotoproduzione singola di pioni. Nell'intervallo di energia  $(250 \div 450)$  MeV i risultati concordano con i valori della sezione d'urto per la fotoproduzione di pioni positivi misurati sperimentalmente. Ad energie maggiori i risultati indicano una resa maggiore di quella prevista per la fotoproduzione doppia di pioni nel particolare canale  $\gamma + p \rightarrow n + \pi^+ + \pi^0$ .